ORIGINAL PAPER

M. Bouroushian · T. Kosanovic · N. Spyrellis

Aspects of ZnSe electrosynthesis from selenite and selenosulfite aqueous solutions

Abstract Cathodic electrodeposition of ZnSe is studied in aqueous acidic selenite ($Se^{(IV)}O_2$) baths of free Zn^{2+} ions and alkaline selenosulfite ($Se^0SO_3^{2-}$) baths of zinc complex ions. The synthesis of polycrystalline, cubic ZnSe by $Se^{(IV)}$-diffusion-controlled electrodeposition from acidic solutions is optimized in terms of selenite concentration, while the effect of Ti, Ni, anodized Ti and CdSe substrates on the obtained layers' growth and structural properties is investigated. Furthermore, the production of stoichiometric though amorphous ZnSe is demonstrated using selenosulfite solutions. The results are valuated by means of X-ray diffraction, scanning electron microscopy and reflectance spectroscopy techniques.

Keywords Zinc selenide · Cathodic electrodeposition · Bilayer growth · Substrate effect · X-ray diffraction

Introduction

On account of its electronic and structural properties, zinc selenide (ZnSe) compound can be advantageously used in the form of thin films, in a variety of advanced electronic and optoelectronic applications. In particular, ZnSe appears to be expedient for the fabrication of blue light photo-electronic diodes, and constitutes one of the basic materials for the construction of heterojunction devices under lattice matching conditions, by adopting suitable alloy systems of other II–VI compounds. Hence, ZnSe can be used as a buffer or window layer in chalcogenide based thin film solar cells. On the basis of band gap energy, ZnSe (2.7 eV)—together with cadmium and zinc oxides and sulfides as well as certain ternaries—is a potential window material while CdSe, CdTe and ternaries of the kind, are used as absorbers.

The various versions of ZnSe cathodic electrodeposition from acidic baths, described previously [1, 2, 3, 4, 5], have been shown to result in the preparation of polycrystalline films suffering from elemental selenium excess and poor integrity, the former strongly determining the latter during deposition. Although removal of Se can be easily accomplished by annealing at low temperatures, the preparation of qualified, compact ZnSe layers is possible only by providing a stoichiometric growth in the first place, since thermal post treatment hardly ameliorates the structure and morphology of the compound film. Thereupon, efforts are directed towards the reduction of free Se co-deposition. For this purpose, a fine control of certain electrolytic parameters seems to be of essential importance. The electrical and temperature conditions have already been optimized [5] for deposits from acidic solutions; in the present work the previously described procedure is improved by varying the bath composition, in particular the selenium precursor content. Further, the type and condition of substrate are proved to substantially influence the electrodeposited layer growth; some interesting results are presented for various substrates. Finally, we bring forward the outcome of a long series of ZnSe electrosynthesis experiments from selenosulfite ions containing alkaline baths.

Materials and methods

Thin films were electroplated mainly potentiostatically at various temperatures in a three-electrode cell fitted to a potentio-scan system (Wenking PGS 81R). Titanium and nickel abraded and polished by 0.25-μm alumina powder, and SnO_2/glass disc electrodes were used as cathodic substrates. Prior to each deposition, Ti was etched by 10% HF for 10 s in order to dissolve the

M. Bouroushian (✉) · T. Kosanovic · N. Spyrellis
General Chemistry Laboratory,
School of Chemical Engineering,
National Technical University of Athens,
Zografos Campus, 157 80 Athens, Greece
E-mail: mirtatb@central.ntua.gr
Tel.: +30-210-7723097
Fax: +30-210-7723088

surface oxide layer. This "activation" also results in roughening of the metal surface [6]. In addition, several Ti specimens were anodized after etching, in either a potentiostatic or a galvanostatic manner, in an electrolyte of 1-M sulfuric acid. The former was carried out under a constant anode-to-cathode voltage drop of 20 or 50 V, applied for 1, 15 or 60 min and the latter was performed by applying constant current densities of 5–10 mA/cm^2 up to a final electrolysis potential of 100 V.

Cathodic electrocrystallization of zinc and cadmium selenides took place from solutions of selenite ($Se^{(IV)}O_2$) and $ZnSO_4$ or $CdSO_4$ precursors, at 85–99 °C, according to a method described in [5, 6, 7]. Mass transfer in this procedure was controlled by a rotating disc electrode setup. Further, electrodeposition was performed from aqueous, near neutral to alkaline solutions (pH 7–13), containing various concentrations of selenosulfite anion ($Se^{(0)}SO_3^{2-}$) and zinc complexes at bath temperatures of 25–85 °C. The $SeSO_3^{2-}$ and Zn complex species were made in situ in separate solutions, which were then mixed. Selenosulfite stock solution was prepared by dissolution of elementary black Se (0.2 M) in a fresh solution of Na_2SO_3 (0.5 M) under an inert argon atmosphere, at 70 °C [8]. Zinc complex solutions were prepared by dissolving $ZnSO_4$ into aqueous media of a strong complexing agent [either nitrilotriacetate (NTA) or ethylendiaminetetraacetate (EDTA)] of limiting excess. Either a rotating or a non-rotating cathode regime was employed. All the above solutions were prepared using as-received analytical grade reagents and water of 18.3 MΩ cm, purified by an ultra-pure water system (Easy Pure Barnstead RF). Electrode potentials refer to a Hg/Hg$_2$SO$_4$ saturated sulfate (SSE) electrode.

The structure of the as-prepared samples was determined by diffractometry in a Siemens D5000 powder X-ray diffraction unit. Compositional data for deposits were obtained by energy dispersive X-ray (EDX) local analysis during electron microscopy in a JEOL JSM 6100 apparatus. Finally, a Hitachi U-4001 spectrophotometer equipped with an integrating sphere was employed to obtain reflectance spectra.

Results and discussion

Acidic solutions. Selenite content effect

Should there exists a sufficiently low concentration of Se precursor in the acidic electrolytic bath, the concentration of the less noble constituent [Zn(II)] being excessive, a chalcogen diffusion-controlled process can be established in solution as the chalcogen ions move towards the rotating cathode. This allows for the formation of well formed, statistically distributed ZnSe tiny crystallites of a dominant sphalerite structure, dispersed within a ZnSe–Se solid phase (Fig. 1) [5]. Growth is rather uncontrollable beyond a certain electrolysis charge of about 3 C, so the deposit thickness is kept in the order of a few hundreds of nm.
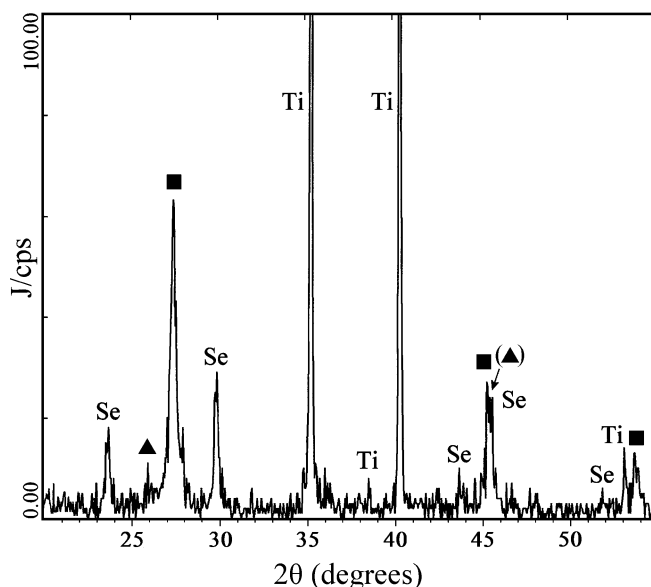

Fig. 1 X-ray diffractogram (CuK$_\alpha$ source) of a deposit prepared on HF-acid-treated Ti at −1.3 V/SSE from a 0.05×10^{-3}-M SeO$_2$, 0.2-M ZnSO$_4$, pH = 3 bath at 85 °C; ZnSe sphalerite (■) and wurtzite (▲) as well as elemental Se (and Ti substrate) reflections are indicated

As verified [5], for potentiostatic deposition on Ti or Ni substrates indifferently, the window for plating parameters in terms of stoichiometry and structure is: deposition potential of −1.1 to −1.3 V vs. SSE; bath pH = 2.5 to 4; [SeO$_2$] = 0.05–0.5 (×10^{-3}) M and [Zn^{2+}] > 0.1 M. Bath temperature of 85–90 °C is an optimal choice to avoid the instability of near boiling baths, though the latter often lead to better results. The as-obtained films are excessive in Se (up to 90 at%) and moderately adherent to the substrate. Chemical etching as well as annealing (at 200 °C in air or at higher temperatures in an inert atmosphere) adjust the stoichiometry, removing excess Se, but without improving the morphology of the ZnSe microcrystalline layers. Thereupon, it is essential to determine the lower limit of operational selenite content in the working bath.

The effect of [SeO$_2$] on film crystallinity is represented in Fig. 2A, which includes sections of recorded XRD diffractograms close to [111] reflection angles as being the most interesting for our purposes; the intensity of cubic (111) peak is taken as a rough measure for obtained crystallinity. It can be seen that an optimal ratio of ZnSe(111)/Se peaks' height is achieved when the selenite concentration in solution is 0.05 mM. Higher selenite content (0.5 mM) promotes the copious deposition of a Se hexagonal phase. A lower content (0.01 mM) leads to the preparation of films with reduced Se excess, although the ZnSe compound obtained is nearly amorphous. Note that the latter contains a small portion of ZnSe wurtzite phase while the increase of [SeO$_2$] in the depositing bath but also buffer substrates as shown below, favor the growth of cubic ZnSe and the [111] orientation as well. Now, since the time required for the intended electrolysis charge to pass through the cell

Fig. 2 XRD patterns (CuK$_\alpha$ source) of deposits prepared with similar electrolysis charge at −1.3 V from a 0.2-M ZnSO$_4$, pH = 3 bath at 85 °C. **A** Samples on HF-acid treated Ti substrates for baths with [SeO$_2$] = 0.5, 0.05 and 0.01 (×10^{-3} M); respective values of FWHM for ZnSe(111): 0.1972°, 0.3678° and 0.9390°. **B** Samples on HF-acid-treated Ti and anodized Ti substrates from a bath with [SeO$_2$] = 0.5×10^{-3} M. **C** Samples on HF-acid-treated Ti and CdSe/Ni substrates from a bath with [SeO$_2$] = 0.5×10^{-3} M. The CdSe/Ni layer was prepared by electrodeposition as described in the text
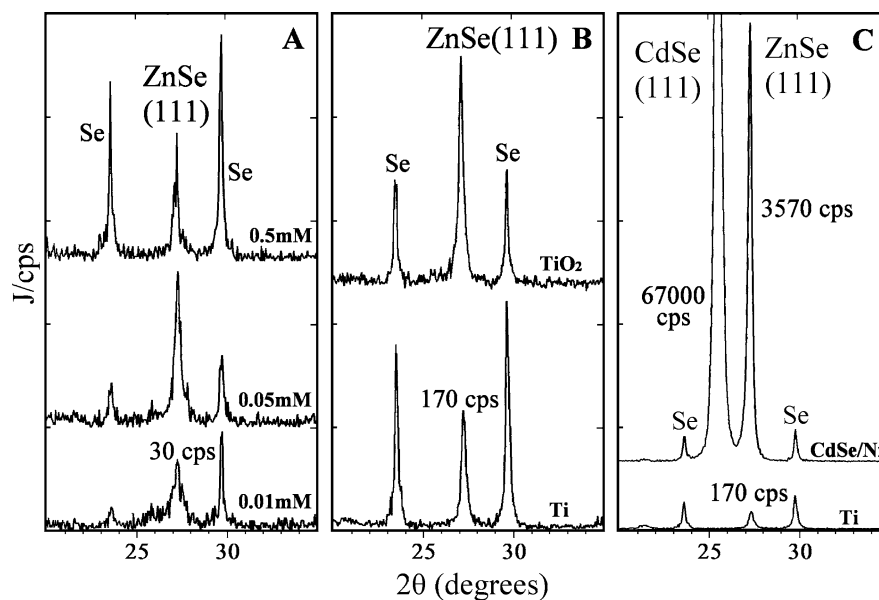
depends on the slow chalcogen-diffusion step, the process is completed much faster with high [SeO$_2$], while concentrations lower than 0.05 mM are hardly operative. The 0.05 mM value makes up the need for decreased required electrolysis time with the need for "soft" growth.

A comparison in terms of full width at half maximum (FWHM) of ZnSe(111) reflection, measured from XRD patterns, is indicative of an increase in ZnSe crystallites' average size with respect to selenite concentration (see Fig. 2A). This trend is not consistent with the increased ZnSe content in the solid at 0.05 mM—according to EDX—but also to the presented XRD intensities. It possibly indicates suppression of ZnSe *nucleation* at higher selenite concentrations (0.5 mM) and also, at the same time, more efficient *growth* of existing crystallites. Both occur because of the Se-rich environment and may be related to the different growth rates of Se and ZnSe phases. The ionic strengths of various solutions are considered to be virtually similar, and determined by the large excess of zinc ions.

Acidic solutions. Effect of Ti, Ni, TiO$_x$ substrates

For constant bath composition, the Zn/Se atom ratio in the solid depends on nucleation and growth conditions, including the deposition substrate effect, which influences the competition between nucleation of Se and ZnSe phases. The nature of the substrate plays a key role in dealing with hydrogen evolution in the range of applied potential as well as in providing specific nucleation conditions.

A smooth Ni substrate, providing a low overpotential to all reducing species, seems initially to induce a higher Zn/Se ratio, which decreases rapidly with layer thickness in accordance with the loss of chalcogen-diffusion control [5]. This is an indication, after all, that an unin-

hibited electrodeposition could be functional. Besides, although a homogeneously nucleated phase often exclusively consisting of hexagonal Se occurs on a pre-etched, rough, Ti substrate in the beginning of deposition (possibly due to the crystallographic match of *c*-axes: 4.6826 for Ti and 4.9536 for Se [JCPDS]), growth establishes a Zn/Se ratio of 0.1 to 0.5; that is, the Zn content may reach about 40 at% though it usually lies at about 20–30 at%.

The influence of the substrate can be effectively demonstrated by performing an oxidation pretreatment of the Ti substrates, since such a modification brings about marked changes in the nucleation process. Anodization of Ti has been used in order to create TiO$_2$ layers a few micrometers thick, containing micropores which act as preferential channels for the current flow during cathodic polarization [7, 9]. Here, it is found that the features of chalcogenide deposits on such substrates are closely connected to the selected anodization mode; thus an optimization of the parameters involved led us to adopt potentiostatic anodizing, preferably for 15 min. As-modified Ti substrates promote the formation of films with an improved ZnSe/Se atom ratio, i.e. lower excess of elemental Se and higher ZnSe(111) reflections beside ZnSe/Ti (Fig. 2B).

In order to explain this effect, a high density of first-born ZnSe nuclei promoted by an increased population of favorable sites associated to the cellular nature of the oxide film may be assumed. The nucleation of a second phase, that of ZnSe, occurs preferentially within the micropores of the substrate, as implied by the experiment. The preference for ZnSe rather than Se may be dictated by the differences in the overpotential between the base and top of the pores as well as by the fact that during deposition the actual Se(+IV) concentration in deeper regions of the TiO$_2$ structure is lowered due to the limitation of surface diffusion, and the excess [Zn(II)] allows for a compact growth of the compound. Further,

structural registration may play an important role; the oxide may account for a release of the strain effects due to lattice mismatch, since oxide ions partly adapt lattice parameters. Note that a mismatch of ~19% is estimated for parameter a between cubic ZnSe and rutile, though ~48% with respect to hexagonal metallic Ti; however, the image is not this simple since anodic TiO_x films contain different anatase/rutile ratios [9]. In any case, after attenuation of the influence of the substrate, Se clusters normally proliferate. Similar phenomena have been observed with roughened deposition substrates for deposition of other chalcogenides [6, 7].

SEM images of ZnSe on microporous oxide films reveal a heterogeneous dispersion of microcrystals incorporated in a matrix rich in Se (Fig. 3). Prominent features in Fig. 3a are greatly enriched in Zn (28–40%) while the surrounding areas are almost pure Se. These ZnSe-rich grains are considered to arise from the substrate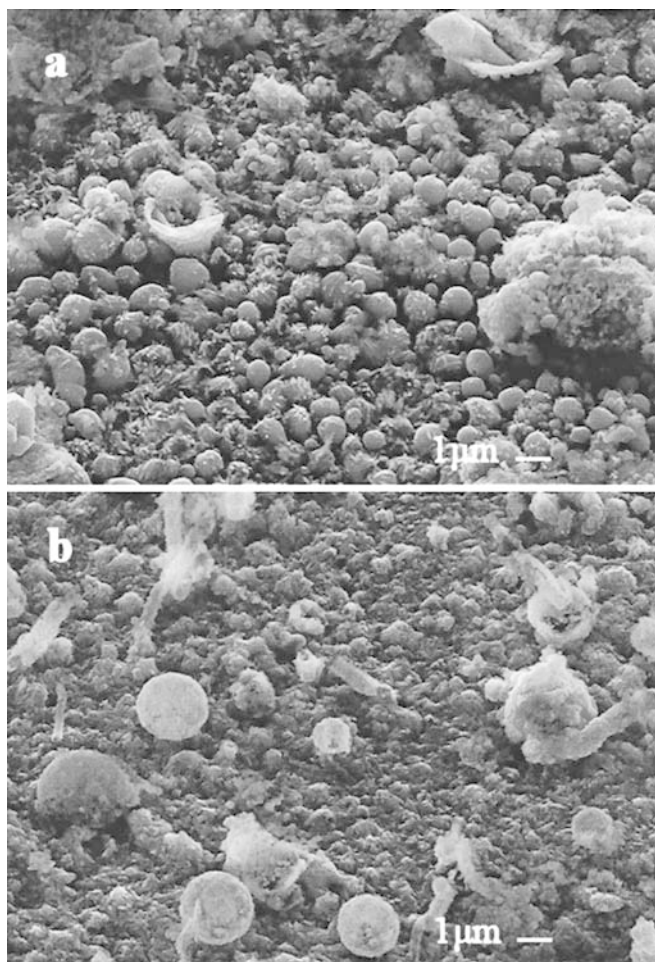 pores by relatively unimpeded growth and to be relatively unaffected by annealing; white spheres in Fig. 3b contain about 47% Zn.

According to spectroscopy, electrolytically grown $ZnSe/TiO_x$ is a well-defined semiconductor when Se, which contributes significantly to the response, is absent. The reflectivity curves included in Fig. 4 show that the decrease in excess of selenium shifts the estimated band gap energy to gradually higher values (curves a, b), which finally reach the characteristic transition of ZnSe (~2.7 eV), after removal of excess Se by annealing or chemical etching (curve c).

Acidic solutions. Growth on CdSe substrate

A CdSe(111) electrode serves as a suitable buffer for adjusting the structure of ZnSe crystallites; many application devices with II–VI materials have been fabricated by epitaxial growth on hetero-substrates of similar chemical type [10].

Cubic polycrystalline, strongly [111] oriented CdSe films were prepared by electrodeposition from an aqueous acidic bath according to a method described e.g. in [6, 7], and used as substrates for ZnSe growth. Representative XRD diagrams obtained for ZnSe/CdSe as well as for ZnSe/Ti samples—prepared under the optimal conditions previously found—are given in Fig. 2C. Evidently, CdSe induces a strong orientation effect on ZnSe crystallites, that is the intensity of ZnSe(111)/CdSe is considerably increased relative to ZnSe(111)/Ti, while ZnSe(220) and (311) reflections (not included in figure) become insignificant. This effect involves an initially strong structural registration of ZnSe on CdSe grains, the growth proceeding in a strictly directional manner. The (111)∥(111) relationship can be attributed to the relatively small mismatch between cubic ZnSe and CdSe lattices, which is estimated to be 6.32%, as well as to the valence and chemical match between the two selenides. The evolution of deposition process with respect to the electrolytic charge passed, and the optical properties of the bilayer, are of great interest and will be reported elsewhere [11].

Fig. 3 SEM micrographs of deposits prepared at −1.3 V from a typical bath 0.05×10^{-3} M in SeO_2: **a** as deposited on anodized Ti substrate, and **b** after heat treatment at 200 °C in air for 30 min. Average atomic composition from EDX: **a** 9% Zn, 91% Se; **b** 42% Zn, 58% Se

Deposition from alkaline selenosulfite solutions

In a selenosulfite $(SeSO_3^{2-})$ based solution, dissolved selenium (0) can undergo electrochemical reduction to highly reactive selenide ions (Se^{2-}). Electroforming of elemental Se is unlikely to occur since high valency Se species such as $Se(+IV)$, which could oxidize the electrogenerated selenide ion, are absent. Besides, any free Se that might form would redissolve in the excess sulfite (SO_3^{2-}). The complexation of zinc is used to avoid the direct reaction of Zn^{2+} with OH^- in the alkaline bath environment. The concentration of free Zn^{2+} ions is then controlled by the excess of complexing agent.

According to voltammetry in solutions of similar ionic strength, the redox potential of Zn^{2+} stays positive

Fig. 4 Reflection spectra of electrolytic layers on anodized Ti: **a**, **b** as deposited; **c** after heat treatment at 200 °C in air for 30 min. Atomic composition from EDX: **a** 9% Zn, 91% Se; **b** 28% Zn, 72% Se; **c** 42% Zn, 58% Se. The estimated band gap widths are 1.90 eV, 1.95 eV and 2.7 eV, respectively. In samples **a** and **b**, the semiconductive Se determines the photoresponse, although the 1.95 eV value for **b** is not considered to be valid for the bulk material, representing instead the response of a superficial layer of the deposit, rich in Se
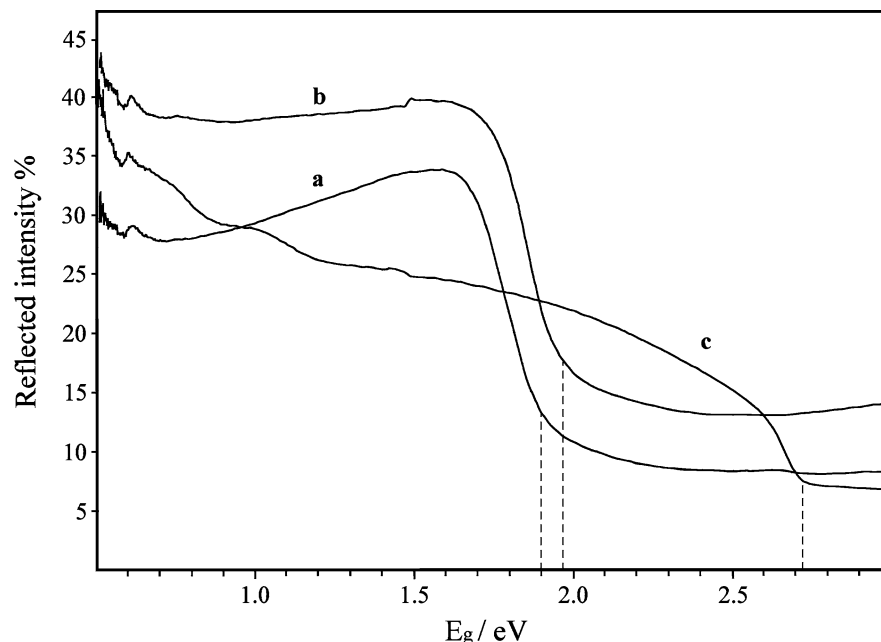
with respect to selenosulfite (Fig. 5), whereas the complexing agent shifts this potential in the cathodic direction (Fig. 5; Zn/NTA$^-$)—this shift has been observed for various metals, complexes and cathodic substrates [12].

Under a constant strong polarization (> -1.8 V), baths with relatively high concentrations of both selenosulfite and zinc complex ions, namely in the range of 0.04–0.1 M, give rise to ZnSe-containing films of an amorphous nature, inasmuch as the cathodic substrate stays un-rotated (Fig. 6A). Note that SnO$_2$/glass substrate promotes better adhesion than HF-treated Ti and Ni. Whatever the electrical parameters are, electrolysis in solutions of medium concentrations, namely 0.02–0.038 M SeSO$_3^{2-}$ and 0.02–0.048 M Zn^{2+}, results in the production of non-coherent films, excessive in elemental

zinc and selenium phases. Finally, no ZnSe compound is detected under all conditions in deposits obtained from solutions containing an excess of zinc complex and low selenosulfite anion concentrations (0.001–0.01 M). Thus, in general, comparable concentrations of precursors may lead to the formation of ZnSe crystallites under a charge-transfer controlled electrolysis regime. Certainly though, a detailed analysis is needed to optimize the results and unravel the formation mechanism.
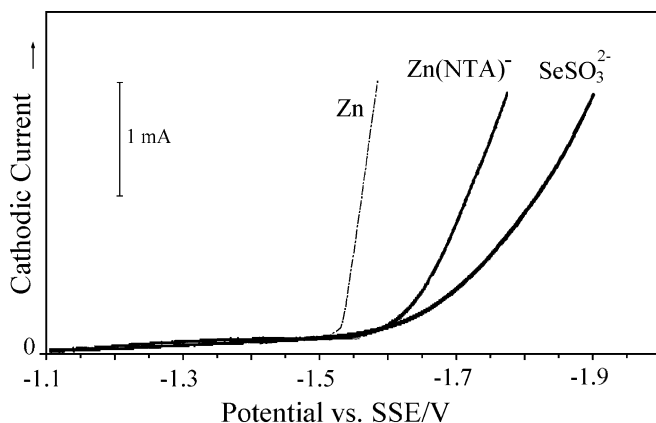
Fig. 5 Cathodic polarization curves of HF-acid-treated Ti electrodes at a scan rate of 5 mV/s in a solution of ZnSO$_4$ and NTA of pH = 9 at 55°C (Zn/NTA$^-$ curve) and a solution of SeSO$_3^{2-}$ and Na$_2$SO$_3$ of pH = 9 at 55°C (SeSO$_3^{2-}$ curve). The standard reduction of Zn^{2+} from acidic solutions is given for reference purposes
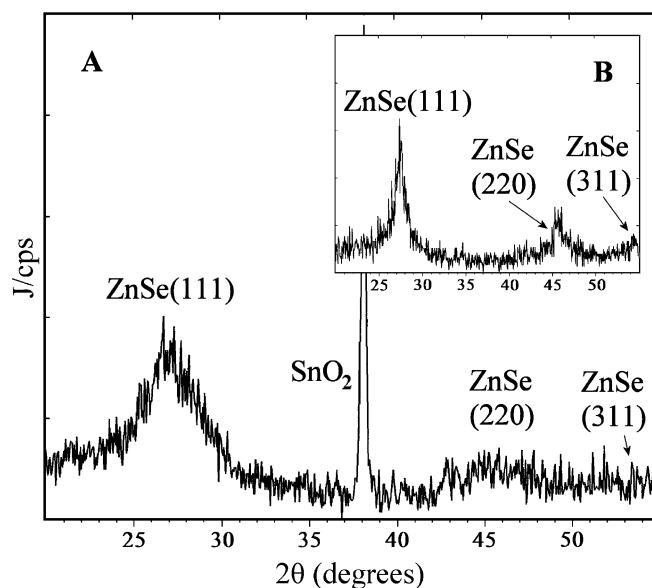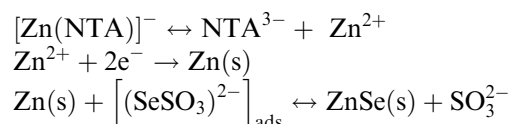
Fig. 6 XRD patterns (CuK$_\alpha$ source) of **A** a layer obtained on an SnO$_2$/glass substrate at −1.8 V from a bath containing 0.1 M ZnSO$_4$, 0.1 M SeSO$_3^{2-}$, 0.1 M EDTA, 0.15 M Na$_2$SO$_3$, pH = 11.5 at 25 °C; **B** the solid residue from a solution containing 0.02 M ZnSO$_4$, 0.02 M SeSO$_3^2$, 0.028 M NTA and 0.08 M Na$_2$SO$_3$ of pH = 10.5 at 85 °C. Hydrazine hydrate was added to this solution in order to speed up precipitation

According to various reports [12, 13, 14, 15, 16] concerning metal selenide synthesis from selenosulfite solutions, the electrochemical formation of ZnSe may involve the following routes:

(i)   Reduction of selenosulfite to selenide ion in the vicinity of the cathode, followed by a homo- or heterogeneous reaction with Zn^{2+} to form ZnSe

(ii) Reduction of Zn^{2+}, followed by a chemical reaction of adsorbed selenosulfite with deposited Zn

(iii) Reduction of a Zn–selenosulfite complex directly to ZnSe.

When the applied potential is sufficiently cathodic to reduce both $SeSO_3^{2-}$ and Zn^{2+}, all the above variants may occur. It appears, though, that better growth is achieved at deposition potentials located between the reduction waves of zinc and selenosulfite. Then the synthetic process unavoidably involves an electroless stage, according to mechanism (ii) above, which can be formulated as follows (for NTA complex):

$$[Zn(NTA)]^- \leftrightarrow NTA^{3-} + Zn^{2+}$$
$$Zn^{2+} + 2e^- \rightarrow Zn(s)$$
$$Zn(s) + \left[(SeSO_3)^{2-}\right]_{ads} \leftrightarrow ZnSe(s) + SO_3^{2-}$$

Actually, in this case, grains of pure ZnSe, often precipitating at the bottom of the cell, are formed (Fig. 6B). This product may arise from the reaction between deposited Zn and adsorbed $(SeSO_3)^{2-}$ on the cathode, but also from a direct homogeneous interaction between species in solution. The addition of suitable reagents, such as hydrazine, favors the latter process.

The selenosulfite-based process is rather complicated and vaguely defined but might be highly rewarding. The type of zinc complex is of central importance and probably the choice of an appropriate complex resulting in a further cathodic shift of zinc redox potential would allow conditions of underpotential deposition, which offers the possibility of better growth control.

Conclusions

The electrochemical preparation of zinc selenide is enriched here with new information, regarding the role of bath composition and deposition substrate. Emphasis is given to the single step formation of rich in ZnSe layers, on account of the shortcoming of any post-deposition treatments.

The typical chalcogen-diffusion-controlled deposition process from acidic solutions, leading to the formation of excessive in Se layers on metallic substrates, is optimized by appropriate control of Se precursor content. Thus, a 0.05×10^{-3} M selenite concentration in the bath is found to fulfil the requirement for a slow deposition with the employed electrolysis duration, in terms of attainable film crystallinity. However, it was verified that a tenfold greater selenite concentration can be maintained without loss in crystallinity or cohesion, simply by controlling the nucleation mode. Thus, the formation of rich in ZnSe phases is promoted by microporous TiO_x substrates produced by anodization. The latter provides an increased population of favorable sites for nucleation.

Both the demonstration of the substrate effect and the practical exploitation in solar cells are fulfilled by electrosynthesizing ZnSe on a suitable semiconducting substrate. A strong epitaxial effect is observed when performing electrodeposition from an acidic bath onto an oriented CdSe[111] substrate. The process results in the formation of well adherent layers rich in ZnSe and exhibiting a sphalerite structure with a pronounced [111] dominant orientation. As far as the authors know no oriented phase of cathodically electrodeposited ZnSe has been observed elsewhere.

Stoichiometric deposition from the outset is possible using the selenosulfite precursor in an alkaline environment; however, this method does not produce compact films of the semiconductor. Amorphous ZnSe is formed during a rather ill-defined procedure involving an electroless reaction at the cathodic surface.

References

1. Mishra KK, Rajeshwar K (1989) J Electroanal Chem 273:169
2. Natarajan C, Sharon M, Lévy-Clément C, Neumann-Spallart M (1994) Thin Solid Films 237:118
3. Chandramohan R, Sanjeeviraja C, Mahalingam T (1997) Phys Status Solidi A 163:R11
4. Riveros G, Gómez H, Henríquez R, Schrebler R, Marotti RE, Dalchiele EA (2001) Solar Energy Mater Solar Cells 70:255
5. Bouroushian M, Kosanovic T, Loizos Z, Spyrellis N (2002) J Solid State Electrochem 6:272
6. Bouroushian M, Charoud-Got J, Loizos Z, Spyrellis N, Maurin G (2001) Thin Solid Films 381:39
7. Bouroushian M, Loizos Z, Spyrellis N (2000) Appl Surf Sci 156:125
8. Gorer S, Hodes G (1994) J Phys Chem 98:5338
9. Deplancke JL, Garnier A, Massiani Y, Winand R (1992) Electrochim Acta 39(8–9):1281
10. Sato K, Seki Y, Matsuda Y, Oda O (1999) J Cryst Growth 197:413
11. Bouroushian M, Kosanovic T, Spyrellis N, to be published
12. Szabo JP, Cocivera M (1986) J Electrochem Soc 133:1247
13. Kitaev GA, Terekhova TS (1970) Russ J Inorg Chem 15/1:25
14. Kutzmutz St, Lang G, Heusler KE (2001) Electrochim Acta 47:955
15. Riveros G, Guillemoles JF, Lincot D, Meier HG, Froment M, Bernard MC, Cortes R (2002) Adv Mater 14(18):1286
16. Riveros G, Lincot D, Guillemoles JF, Henríquez R, Schrebler R, Cordova R, Gomez H (2003) J Electroanal Chem 558:9